

Electroactuation with Single Charge Carrier Ionomers

Alpha A. Lee and Alexei A. Kornyshev*

Department of Chemistry, Faculty of Natural Sciences, Imperial College London, SW7 2AZ, UK

Ralph H. Colby

Department of Chemistry, Faculty of Natural Sciences, Imperial College London, SW7 2AZ, UK and

Department of Materials Science and Engineering and Materials Research Institute,

The Pennsylvania State University, University Park, PA 16802, USA

A simple theory of electromechanical transduction for single-charge-carrier double-layer electroactuators is developed, in which the ion distribution and curvature are mutually coupled. The obtained expressions for the dependence of curvature and charge accumulation on the applied voltage, as well as the electroactuation dynamics, are compared with literature data. The mechanical- or sensor-performance of such electroactuators appears to be determined by just three cumulative parameters, with all of their constituents measurable, permitting a scaling approach to their design.

Electro-mechanical materials have long intrigued physicists. Such materials can serve as sensors and transducers (where mechanical stimulation generates a voltage) or can function as electroactuators where voltage generates a mechanical response (for review see [1–3]). A class of such materials, called Ionomeric Polymer Metal Composites (IPMC), is based on the motion of ions of one sign in an elastic polymer membrane enclosed between two bendable electrodes. Applied voltage causes mobile ions to accumulate near the oppositely charged electrode, forming an electrical double layer that expands the membrane and a depletion layer at the opposite electrode that contracts the membrane, causing bending (Fig. 1).

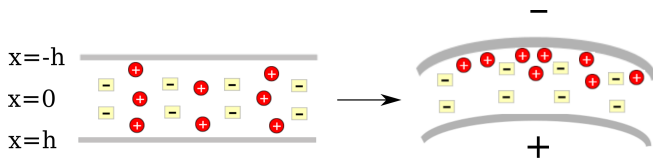


FIG. 1. Electroactuators based on mobile cations: redistribution of cations in the ionomer membrane between two flexible electrodes causes bending [3].

Early materials were swollen with polar solvents such as water, and were often single-ion conductors [4–6]. More recently, these volatile solvents were replaced with ionic liquids [7–10] to eliminate evaporation problems, but necessarily creating dual-ion conductors that often bend first forward and later backwards under a constant applied voltage [11]. Sophisticated models for ionic actuation with multiple sorts of charge carriers have been developed [12–15]. Those pioneering works, however, did not incorporate the feedback of mechanical deformation on the ionic charge distribution, which impedes their application for a description of the sensing function of electroactuators. The complexity of those models make them impractical for direct use in designing new actuators.

We focus here on a simpler system, containing only one mobile charge carrier [16] (for optimal electroactu-

ation) for which it was straightforward to incorporate the stress-to-voltage feedback, as well as the volume of ions in electrical double layers. The analysis shows which physical characteristics determine the response and how they can be grouped into only two dimensionless cumulative parameters to describe the beam deflection under the applied voltage, with a third cumulative parameter determining the time scale of bending dynamics. This grouping reveals the interrelations between the physical characteristics, instructs what should be measured to predict electroactuator performance, and makes possible a scaling approach to their design.

Statics - The equilibrium properties of this system can be derived by minimising the free energy functional

$$\mathcal{F}[\psi, \rho, \kappa] = \mathcal{S} \int_{-h}^h dx \left[-\frac{\varepsilon}{8\pi} \left(\frac{d\psi}{dx} \right)^2 + e\rho\psi + g - K\nu\rho\kappa x \right] + \frac{1}{3}\mathcal{S}_0 E h^3 \kappa^2, \quad (1)$$

$$g = k_B T \left[c_+ \ln\left(\frac{c_+}{c_{\max}}\right) + (c_{\max} - c_+) \ln\left(1 - \frac{c_+}{c_{\max}}\right) \right] \quad (2)$$

where \mathcal{S} and \mathcal{S}_0 are the contact surface area and projected area of the electrodes, respectively, [17]; h is the half-separation of electrodes (positioned at $x = -h$ and $x = h$); ε is the dielectric permittivity (assumed to be constant across the membrane); $\psi(x)$ is the electrostatic mean-field potential distribution; $\rho(x) = c_+(x) - c_0$ is the local excess number density of cations; K is the bulk modulus of the polymer matrix; ν is the excess volume associated with each cation (including solvation shell, if present); κ is the curvature of the actuator; E is the elastic modulus of the whole construction including the metallic plates, which in the first approximation can be considered as the volume weighted average of the Young's moduli of the metal and the polymer [12]; c_{\max} is the maximal local concentration of cations [18].

The first term in Eq. 1 is the self-energy of the electric field plus that of the battery, keeping a defined potential

across the plates. The second term accounts for the electrostatic energy of all ions interacting with each other and with the external field. The third term (see Eq. 2) is the entropy of the standard “lattice-gas model” [19], including the volume of ions [20]. The fourth term is the pressure-volume work that provides the coupling between mechanical bending and the ion concentration profile. Indeed, $Kv\rho$ is the pressure exerted by ions and κx the elongation of the device due to curvature at a distance x away from the centre ($x > 0$ in extension; $x < 0$ in compression). This effective pressure-volume work characterises ion-induced *swelling*. This term is proportional to the sum of first moments of the charge distributions at each electrode, reflecting the fact that the more polarized the charge distribution, the more favourable bending is and vice versa. The fifth term, outside the integral, is the energetic cost of bending an Euler-Bernoulli beam.[21] Note that the beam is assumed to be much longer than its width, precluding Gaussian curvature with only 1-dimensional bending.

All in all, Eqs. 1,2 describe several competing physical effects: the electrostatic and entropic costs of building up ions near one electrode and depleting them at the other. Bending relieves the energy of charge accumulation but the extent of bending is inhibited by the mechanical energy needed to deform the material.

Minimising the free energy functional (Eqs. 1,2) with respect to ρ , constraining the total number of ions, gives the electrochemical potential of the mobile ions $\mu_+ = e\psi + k_B T \ln[c_+/(c_{\max} - c_+)] - Kv\kappa x$. By equating μ_+ to its value in the bulk, [22] $\mu_0 = k_B T \ln[c_0/(c_{\max} - c_0)]$, we obtain the cation distribution (Fermi-like if $\kappa = 0$) [19]

$$c_+ = \frac{c_{\max}}{\left[\frac{c_{\max}}{c_0} - 1 \right] \exp \left[\frac{e\psi - Kv\kappa x}{k_B T} \right] + 1}. \quad (3)$$

Consequently, minimisation of Eqs. 1 and 2 gives a (dimensionless) modified Poisson-Fermi equation

$$\frac{d^2 y}{dX^2} = \frac{(1 - \gamma)(e^y - 1)}{(1 - \gamma)e^y + \gamma}, \quad (4)$$

with dimensionless variables $X \equiv x/l_D$, $y \equiv e\psi/k_B T - p\kappa X l_D$ where $p \equiv Kv/k_B T$, ion crowding parameter $\gamma \equiv c_0/c_{\max}$, Debye length $l_D = (4\pi l_B c_0)^{-1/2}$ and Bjerrum length $l_B = e^2/\varepsilon k_B T$. Equation 4 is solved with boundary conditions $y' = y = 0$ at $x = 0$, corresponding to vanishing electric field and potential in the bulk. These conditions are true for widely separated electrodes, so that the electrical double layer does not overlap the depletion layer, maintaining electroneutrality in the bulk; warranted unless the membrane is nanoscale thin. One can then combine two semi-infinite solutions corresponding to the anode and cathode. Taking the first integral of Eq. 4, gives the expression for the electric field:

$$\left| \frac{dy}{dX} \right| = \sqrt{y + \frac{1}{\gamma} \ln(\gamma e^{-y} - \gamma + 1)}. \quad (5)$$

Minimising Eq. 1 with respect to κ with $H \equiv h/l_D$ and $\tilde{\rho} \equiv (c_+/c_0) - 1$, gives the dimensionless curvature:

$$\begin{aligned} \varkappa \equiv \kappa h &= \frac{3vK}{2Eh^2} \frac{S}{S_0} l_D^2 c_0 \int_{-H}^H X \tilde{\rho} dX \\ &\approx \frac{3vK}{2Eh} \frac{S}{S_0} l_D c_0 \left(\int_0^H \tilde{\rho} dX - \int_{-H}^0 \tilde{\rho} dX \right). \end{aligned} \quad (6)$$

The approximate equality is justified as the range of the charge density variation is much shorter compared to the separation between the electrodes [23]. Hence, $\varkappa \sim Q$ where Q is the charge per unit cross-section area stored in both the double layer and depletion layer, consistent with experimental results [5]. The integrals in Eq. 6 can then be evaluated using the Gauss law [24] which relates surface charge densities at each of the electrodes to electric inductions. Since the electrical induction (Eq. 5) contains itself \varkappa through the definition of y , a transcendental equation for \varkappa emerges:

$$\begin{aligned} \varkappa = \alpha \left\{ \sqrt{2 \left[V_1 - p\varkappa + \frac{1}{\gamma} \ln(\gamma e^{-V_1 + p\varkappa} - \gamma + 1) \right]} \right. \\ \left. + \sqrt{2 \left[-V_2 + p\varkappa + \frac{1}{\gamma} \ln(\gamma e^{V_2 - p\varkappa} - \gamma + 1) \right]} \right\} \end{aligned} \quad (7)$$

Here α , the dimensionless *electroactuation number*, is the key cumulative parameter for the actuation strength [25].

$$\alpha \equiv \frac{3K}{2} \frac{l_D}{E} \frac{S}{h} \frac{S_0}{c_0 v} \equiv \frac{3}{4\sqrt{\pi}} \frac{K}{E} \frac{S}{S_0} \frac{v}{h} \frac{c_0^{1/2}}{l_B^{1/2}}. \quad (8)$$

The response vanishes when the membrane is soft or the plates are rigid ($K/E \rightarrow 0$). Here, the dimensionless potential drops V , V_1 and V_2 are, respectively, the total voltage, and the potential drops near the positive and negative electrodes, all normalized to $k_B T/e$, obtained via equating the induction, thus the surface charge density, on both electrodes (this transforms the system into a constant voltage ensemble):

$$V_1 = V - V_2 = p\varkappa + \ln \frac{1 - \exp[(1 - \gamma)(V - 2p\varkappa)]}{(1/\gamma - 1)(\exp[-\gamma(V - 2p\varkappa)] - 1)}. \quad (9)$$

Expanding Eq. 7 in the low voltage regime gives $V_1 \approx V_2 \approx V/2$ and $\varkappa \approx \alpha \sqrt{(1 - \gamma)V}$. In the opposite large voltage limit, $V_1 \approx (1 - \gamma)V$ and $\varkappa \approx \alpha \sqrt{8(1 - \gamma)V}$. Figure 3 shows the full numerical solution of Eq. 7, where these two limits are recovered. This solution is replicated by the interpolation formula

$$\varkappa = \alpha \sqrt{1 - \gamma} \frac{V}{\sqrt{\frac{V}{8} + 1}} \quad (10)$$

matching the two limits. As seen from Eq. 10, the crossover from linear to non-linear regimes occurs at

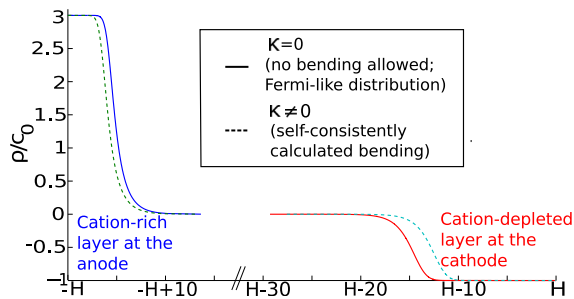


FIG. 2. Bending reduces the charge separation between the electrodes. Charge density profiles (Eq. 3) are plotted as functions of the distance from the corresponding electrode within the proposed self-consistent theory at applied 4 Volts and for $\alpha = 1.3 \times 10^{-3}$, $\gamma = 0.25$ and $S/S_0 = 5$. $2H \equiv 2hl_D^{-1}$, is the membrane thickness measured in units of Debye length.

$V = 8$. At 300K, this corresponds to 0.2 Volts (see Fig. 3). This crossover has been observed experimentally in single-mobile-charge systems [26, 27] and was rationalized in ref [28]. Rearranging Eq. 10 yields a simple law for the treatment of experimental data: $(V/\varkappa)^2 = \alpha^2 (1 - \gamma) (1 + \frac{V}{8})$ which gives a straight line plotting $(V/\varkappa)^2$ vs V . Experimental tests of this law and its 1/8 ratio between the slope and intercept are needed.

To illustrate how the full solution of Eq. 7 works, consider an example: $1 \mu\text{m}$ thick Nafion of volume fraction 0.6, with volume fraction of mobile cationic counterions 0.1 and ethylene carbonate solvent 0.3 with "typical" physical characteristics (dielectric constant $\varepsilon \sim 10$ [29], ion excess volume $v = 0.3 \text{ nm}^3$ [30], ion crowding parameter $\gamma = 0.25$ [31] and $K/E = 13$ for Nafion [32]).

Figure 2 shows that the effect of curvature on the concentration profile is to reduce ion polarization at the electrodes. This is expected, as bending relieves the steric and electrostatic strain induced by the accumulation and depletion of mobile ions near the electrodes. Bending opens extra volume close to the negative electrode, lowering the local concentration of cations. Conversely at the positive electrode, bending decreases the extent of the depletion layer.

Figure 3 demonstrates that larger electrode/membrane contact area and larger volume of the charge carrier enhance bending. More charge is stored for higher surface area electrodes and crowding in the double layer increases with ion size [35]. To achieve a substantial curvature of $\kappa = 1 \text{ cm}^{-1}$ at an applied voltage of 4V, assuming $\gamma = 0.25$, α/h must be greater than 0.03 cm^{-1} . Using the above physical characteristics, the separation between the electrodes must be less than $10 \mu\text{m}$.

This simple model has no hysteresis or dissipation effects; the electroactuator response is fully reversible. Experimentally, hysteresis may occur due to non-idealities such as Joule heating, leakage of solvent outside the electrode, irreversible mechanical deformation of the ionic

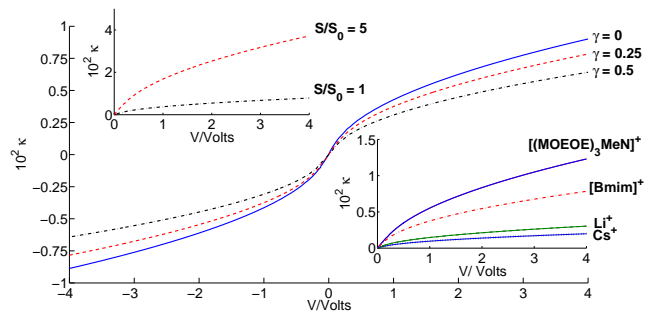


FIG. 3. Dimensionless curvature \varkappa as a function of applied voltage. The main panel demonstrates the effect of ion crowding parameter γ at fixed α . The insets show two of the many ways to vary α ; the effects of roughness factor S/S_0 and of the effective volume of ion for $\gamma = 0.25$, $S/S_0 = 1$ and $v = V_{[\text{Bmim}]^+}$. The volumes of ions used are $V_{[\text{Bmim}]^+} = 0.3 \text{ nm}^3$ [33], $V_{[(\text{MOEOE})_3\text{MeN}]^+} = 1 \text{ nm}^3$ [28], and hydrated ion volumes $V_{\text{Li}^+} = 0.23 \text{ nm}^3$, $V_{\text{Cs}^+} = 0.15 \text{ nm}^3$ [34]. Other physical characteristics are the same as Figure 2.

polymer metal composite [36, 37] and the current from trace water hydrolysis. Nanoporous electrodes [38, 39] are also not considered; surface roughness is assumed to occur on a scale much larger than the Debye length.

Dynamics - The simplest results can be obtained assuming: (i) the mechanical response time of the polymer is much faster than the charging of the double layer, (ii) the height of the electrode roughness is much smaller than the electrode-electrode separation and (iii) the dimensions of all channels are much larger than both the hydrated ion size and the Debye length. In this case, the response dynamics are solely determined by the migration of ions through the bulk and an equilibrium-like charging of the electrical double layers. The theory of double layer charging in single-mobile-charge-carrier systems has been considered in detail [19, 40]. Applying this to the case of electro-actuation, in response to a dimensionless step potential $U_0 (\equiv eV_0/k_B T)$ imposed at $t = 0$, we find an equation for $\varkappa(t)$ [41],

$$t = \frac{\tau}{\alpha} \int_0^{\varkappa(t)} \frac{d\varkappa}{U_0 - V(\varkappa)}. \quad (11)$$

Here $\tau = R_0 C_0$; $R_0 = 2h/(S_0 \sigma) = 2hk_B T/(S_0 c_0 e^2 D)$ is the resistance of the bulk (σ is the ionic conductivity and D is the diffusion coefficient of the ion); $C_0 = \varepsilon S/(8\pi l_D)$ is the linear Debye capacitance, giving

$$\tau = \frac{hl_D}{D} \frac{S}{S_0}. \quad (12)$$

Equation 11 is solved analytically in the limits of linear response ($U_0 < 8$) and strongly nonlinear response:

$$\varkappa(t) = \alpha \sqrt{1 - \gamma} \left\{ U_0 \left(1 - \exp \left[\frac{-t}{\tau \sqrt{1 - \gamma}} \right] \right) \right\} \quad \text{for } U_0 < 8\sqrt{8U_0 \tanh} \quad (13)$$

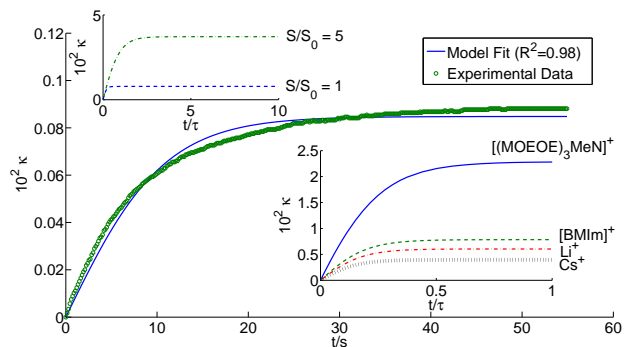


FIG. 4. The main panel shows fitting of experimental data taken from refs [6, 14] with the non-linear response case of Eq. 13. There, a rectangular Nafion membrane of dimension $4 \times 35 \times 0.2\text{mm}$ was coated with a platinum electrode and then treated with a thin gold overlayer. The counterion was Li^+ with glycerol as solvent. A 1V applied potential ($U_0 = 40$) induced bending. Assuming $\gamma = 0.25$, the two-parameter fit to Eq. 13 yields $\alpha = 5.6 \times 10^{-5}$ and $\tau = 28\text{s}$. The two insets show the effects of the electrode contact surface area and ion size on actuation response, from a 4V step voltage (see text and the Figure 3 caption for other parameters used).

The two forms coincide at short times, where the initial rate of bending $\alpha U_0/\tau$ is independent of γ , since crowding of ions requires time to develop. The maximum final bending (Eq. 10) scales as $\alpha\sqrt{1-\gamma}$ which is maximal at $c_0 = c_{\text{max}}/2$ (or $\gamma = 1/2$). Hence, a vital prediction of our model is that single-ion actuators could be improved by roughly doubling the ion exchange capacity [42] of Nafion ionomers. The relation between excess ion volume and actuation rate can be obtained by noting that in the linear response regime, $\varkappa \sim vt/R_0$ with $R_0 \sim v^{1/3}$ [43]. This gives the counter-intuitive prediction $\varkappa \sim v^{2/3}t$ that the actuation becomes more rapid with larger ions! In the main part of Figure 4, the full $\varkappa(t)$ curve, calculated via Eq. 13, is compared with experimental data [6, 14].

Conclusion - A self-consistent theory of single-ion conducting electroactuators is presented, in which the curvature is considered on the same footing as the concentration profiles, modelling both actuation and sensing. The model assumes a strong coupling of ion build-up and depletion with local volume that forces bending. The theory reveals the roles of all physical characteristics but most importantly, they group themselves into three cumulative parameters: (i) dimensionless response coefficient - the *electroactuation number* α (Eq. 8), (ii) ion crowding parameter γ and (iii) the relaxation time τ for dynamics (Eq. 12). These three parameters have clear constituents, each of which can be independently measured or estimated. Other results are as follows:

- At large voltages, both curvature and charge accumulation increase as \sqrt{V} , owing to ion crowding.
- For a given voltage, increasing the surface roughness, volume of ion and decreasing the electrode-electrode sep-

aration all increase bending.

- Plotting experimental data as $(V/\varkappa)^2$ vs. V is predicted (Eq. 10) to give a straight line with a slope 8 times smaller than the intercept.
- The dynamic response is described by simple analytical formulae (Eqs. 12 and 13).
- Electroactuation number α allows a scaling approach for rational design of electroactuators. [44]

We thank A. Isaacs, S. Kondrat and Q. Zhang for insightful discussions. This work is supported in part by the Grant EP/H004319/1 of the Engineering and Physical Science Research Council, Leverhulme Visiting Professorship to RHC, as well as U.S. Army Research Office under Grant No. W911NF-07-1-0452 Ionic Liquids in Electro-Active Devices (ILEAD) MURI.

* a.kornyshev@imperial.ac.uk

- [1] K. Oguro, Y. Kawami, and H. Takenaka, Journal of Micromachine Society **5**, 27 (1992).
- [2] M. Shahinpoor, Y. Bar-Cohen, J. Simpson, and J. Smith, Smart Mater. Struct **7**, R15 (1998).
- [3] Y. Bar-Cohen and Q. Zhang, MRS Bull. **33**, 173 (2008).
- [4] Y. Abe, A. Mochizuki, T. Kawashima, S. Yamashita, K. Asaka, and K. Oguro, Polymer. Adv. Tech. **9**, 520 (1998).
- [5] B. Akle, D. Leo, M. Hickner, and J. McGrath, J. Mater. Sci. **40**, 3715 (2005).
- [6] K. M. Farinholt and D. J. Leo, J. Intel. Mater. System and Structures **18**, 677 (2007).
- [7] M. Bennett and D. Leo, Sensor Acutat. A-Phys **115**, 79 (2004).
- [8] J. Wang, C. Xu, M. Taya, and Y. Kuga, Smart Mater. Struct **16**, S214 (2007).
- [9] A. J. Duncan, D. J. Leo, and T. E. Long, Macromolecules **41**, 7765 (2008).
- [10] S. Liu, W. Liu, Y. Liu, J.-H. Lin, X. Zhou, M. J. Janik, R. H. Colby, and Q. Zhang, Polym. Int. **59**, 321 (2010).
- [11] J. Lin, Y. Liu, and Q. Zhang, Polymer **52**, 540 (2011).
- [12] S. Nemat-Nasser, J Appl. Phys. **92**, 2899 (2002).
- [13] S. Nemat-Nasser and Y. Wu, Smart Mater. Struct **15**, 909 (2006).
- [14] K. M. Farinholt and D. J. Leo, J. Appl. Phys. **104**, 14512 (2008).
- [15] D. Pugal, K. Jung, A. Aabloo, and K. J. Kim, Polym. Int. **59**, 279 (2010).
- [16] Single-charge-carrier ionomers are usually made of poly-electrolyte membrane with side-chains terminated by acid groups which dissociate leaving anionic groups bound to the side chains. The mobile protons can be chemically exchanged for various cations.
- [17] For a poor contact between the electrode and the membrane, it is possible that $S < S_0$. For a rough electrode surface with good contact, $S > S_0$.
- [18] Gaussian units are used throughout the article.
- [19] A. Kornyshev and M. Vorotyntsev, Electrochim. Acta **26**, 303 (1981).
- [20] In the dilute (Gouy-Chapman, non-interacting) limit $c_0 \ll c_{\text{max}}$, Eq. 2 reduces to the entropy density of an

- ideal gas $g_{GC} = k_B T [c_+ \ln(c_+/c_0) - c_+]$.
- [21] L. D. Landau and E. M. Lifshitz, *Theory of Elasticity*, 3rd ed. (Pergamon Press, 1986).
- [22] As the separation between the electrodes is much greater than the width of the double layers at the electrodes, the bulk of the system is electroneutral and is characterised by constant chemical potential.
- [23] Equation 6 is equivalent to the assumption that bending moment $\sim \int_{-H}^H X \tilde{\rho} dX$ [45, 46].
- [24] L. D. Landau, E. M. Lifshitz, and L. P. Pitaevskii, *Electrodynamics of Continuous Media* (Elsevier SCI LTD, 1984).
- [25] The second equality is obtained using the definition of Debye length l_D , yielding $\alpha \sim c_0^{1/2}$.
- [26] C. R. Mariappan, T. P. Heins, and B. Roling, *Solid State Ionics* **181**, 859 (2010).
- [27] T. Wallmersperger, B. J. Akle, D. J. Leo, and B. Kroepelin, *Compos. Sci. Technol.* **68**, 1173 (2008).
- [28] G. J. Tudryn, W. Liu, S.-W. Wang, and R. H. Colby, *Macromolecules* **44**, 3572 (2011).
- [29] The dielectric constant of the system is estimated by the effective medium theory as for a composite mixture of non-polar (polymer) and polar (solvent) phases using the Bruggeman formula [47].
- [30] The volume of the ion is taken as the volume of 1-butyl-3-methylimidazolium (BMIm) [33], a typical bulky ion used in electroactuators, $v = 0.3 \text{ nm}^3$.
- [31] The ion crowding parameter γ is estimated here from the simple relation $\gamma \sim \frac{\varphi_{ion}}{\varphi_{ion} + \varphi_{solv}} = 0.25$ where φ_{solv} and φ_{ion} are the volume fractions of solvent and charge carrier respectively, as densest packing of ions near the electrode correspond to total displacement of solvent. In typical conditions $0.2 \leq \gamma \leq 0.3$.
- [32] J. Li and S. Nemat-Nasser, *Mech. Mater.* **32**, 303 (2000).
- [33] S.-W. Wang, W. Liu, and R. H. Colby, *Chem. Mat.* **23**, 1862 (2011).
- [34] J. O. Bockris and P. P. S. Saluja, *J. Phys. Chem.* **76**, 2140 (1972).
- [35] Compression of the ionic cloud is necessary for the generation of stress and the ion crowding parameter γ governs the compressibility thus controls the actuation performance of the system. Indeed at $\gamma = 1$, distribution of ions cannot compress and the actuation response is zero.
- [36] M. Shahinpoor and K. J. Kim, *Smart Mater. Struct.* **10**, 819 (2001).
- [37] *Quasi-static Positioning of Ionic Polymer-Metal Composite (IPMC) Actuators* (Proceedings of IEEE/ASME International Conference on Advanced Intelligent Mechatronics, 2005).
- [38] S. Kondrat and A. Kornyshev, *J. Phys.: Condens. Matter* **23** (2011), ARTN 022201.
- [39] S. Kondrat, N. Georgi, M. V. Fedorov, and A. A. Kornyshev, *Phys. Chem. Chem. Phys.* **13**, 11359 (2011).
- [40] D. C. Grahame, *Chemical Reviews* **41**, 441 (1947).
- [41] The equations $V(\varkappa) \approx \varkappa^2 / [8\alpha^2(1 - \gamma)]$ at large voltages and $V(\varkappa) \approx \varkappa / [\alpha\sqrt{1 - \gamma}]$ at low voltages are used.
- [42] Ion exchange capacity refers to the density of ionic groups attached to the polymer (and their counterions) in any single-ion conducting ionomer, see J. A. Kerres, *J. Membrane Sci.* **185**, 3 (2001).
- [43] The latter is Stoke's Law type scaling. It may break down at the limit of large concentration of ions and non-spherical ions [48].
- [44] This is applicable in full to the equilibrium response. The effects shown in the insets of Fig. 3 can be accounted for by pure rescaling of α . It is trickier in dynamics, however. Electroactuation number α does determine the electroactuation amplitude, but only a subset of the physical characteristics that comprise α enter the characteristic time τ , which also involves the ion diffusion coefficient D , see Eq. 12.
- [45] M. Porfiri, *J. Appl. Phys.* **104** (2008), ARTN 104915.
- [46] T. Wallmersperger, D. J. Leo, and C. S. Kothera, *J. Appl. Phys.* **101** (2007), ARTN 024912.
- [47] D. Bergman, *Phys. Rep.* **43**, 378 (1978).
- [48] M. A. Vorotyntsev, V. A. Zinovyeva, and M. Picquet, *Electrochim. Acta* **55**, 5063 (2010).